Polymer Cookery: Influence of Polymerization Conditions on the Performance of Molecularly Imprinted Polymers

Sergey A. Piletsky,*,† Elena V. Piletska,† Kal Karim,† Keith W. Freebairn,‡ Coulton H. Legge,‡ and Anthony P. F. Turner†

Institute of BioScience and Technology, Cranfield University, Silsoe, Bedfordshire, MK45 4DT, UK, and GlaxoSmithKline Research and Development, Gunnels Wood Road, Stevenage, Herts, SG1 2NY, UK

Received April 8, 2002; Revised Manuscript Received June 25, 2002

ABSTRACT: A set of polymers has been imprinted with (−)-ephedrine at six different temperatures, ranging from −30 to +80 °C. Polymer affinity and specificity were observed to be strongly dependent on the polymerization temperature. The experimental results suggest that the polymer is able to "memorize" the temperature used in the polymerization process in a manner similar to previously documented MIP "memory" effects for the template and polymerization solvent. In a study of the effect of temperature on retention and selectivity in HPLC (using the MIP as a column packing), a clear gradient change in the Van't Hoff plots was observed at 20−30 °C. This indicates a transition in binding mechanism from exothermic at higher temperatures to endothermic at lower temperatures. These results, supported by the evidence of template-induced MIP swelling, are interpreted in terms of desolvation and conformational changes in the polymers induced by the interaction with the template.

Introduction

The development of synthetic receptors capable of recognizing small organic molecules is an important area in fundamental and applied sciences. Several synthetic approaches are available for the preparation of synthetic receptors; these include rational, combinatorial syntheses, and molecular imprinting.[1] The concept of molecular imprinting in organic polymers was introduced by Wulff in 1972.[2] The process involves the formation of a molecular complex between functional monomers and a target compound (template). Subsequent thermal or photoinitiated radical polymerization in the presence of cross-linker results in a "freezing" of this complex inside the three-dimensional polymer network. Removal of the template from the polymer leaves cavities or imprints with the shape and orientation of the functional groups complementary to those of the template molecule. The preservation of the structure of the monomers−template complex during the polymerization step is a crucial element, which determines the success of the imprinting procedure.

The stability of monomers−template complexes and their type and concentration depend on the polymerization conditions. The complex formation phase is under thermodynamic control, and its energetics can be described by the equation[3]

$$\Delta G_{\text{bind}} = \Delta G_{\text{t+r}} + \Delta G_{\text{r}} + \Delta G_{\text{h}} + \Delta G_{\text{vib}} + \sum \Delta G_{\text{p}} + \Delta G_{\text{conf}} + \Delta G_{\text{vdW}} \quad (1)$$

where the Gibbs free energy changes are ΔG_{bind} the complex formation, $\Delta G_{\text{t+r}}$ the translational and rotational, ΔG_{r} the restriction of rotor upon complexation, ΔG_{h} the hydrophobic interactions, ΔG_{vib} the residual soft vibrational modes, $\sum \Delta G_{\text{p}}$ the sum of interacting polar group contributions, ΔG_{conf} the adverse conformational changes, and ΔG_{vdW} the unfavorable van der Waals interactions.

Attempts have been made in the past to use thermodynamic calculations, sometimes in combination with NMR or UV titration, for the analysis of monomers−template complexation processes and the prediction of MIP performance.[4] To be correct, this modeling needs to satisfy three conditions: the structure of the monomers−template complex existing in solution prior to polymerization should remain the same after the saturation of double bonds and formation of polymer chains; the temperature used in the modeling should match the actual temperature developed during polymerization; the polarity of the monomer mixture should be the same as the polarity of the imprinted cavities of the resulting polymer. Because of obvious difficulties in satisfying these criteria, primarily due to the absence of information about the real system, the practical application of modeling remains limited. The general considerations listed above, however, still remain relevant, and conditions that enhance monomers−template complexation are important for successful imprinting.

The polymer affinity and specificity rely significantly on the right choice of monomers, cross-linker, solvent, and polymerization temperature. Monomers are selected on the basis of the strength of their interactions with the template, which contribute to $\sum \Delta G_{\text{p}}$, ΔG_{h}, and $\Delta G_{\text{t+r}}$ in eq 1. This selection can be performed empirically by testing a series of polymers prepared using different monomers or rationally by computational screening of a virtual library of functional monomers.[5] The beneficial role of the cross-linker in covalent and noncovalent imprinting was studied previously and was explained in terms of preserving the structure of the imprints formed.[6] Solvent can change the entropy and enthalpy of the complexation ($\sum \Delta G_{\text{p}}$, ΔG_{h}) and can improve unfavorable van der Waals interactions (ΔG_{vdW}) through an effective solvation process. In addition to the thermodynamic contributions, solvent influences mass transfer by affecting polymer morphology.[7] Temperature has a complex effect on monomer−template and polymer−template interactions. Lower temperature should be

† Cranfield University.
‡ GlaxoSmithKline Research and Development.
* To whom correspondence should be addressed: Tel +44 (0)-1525 863584, fax +44 (0)1525 863533, e-mail S.Piletsky@cranfield.ac.uk.

10.1021/ma0205562 CCC: $22.00
Published on Web 08/08/2002

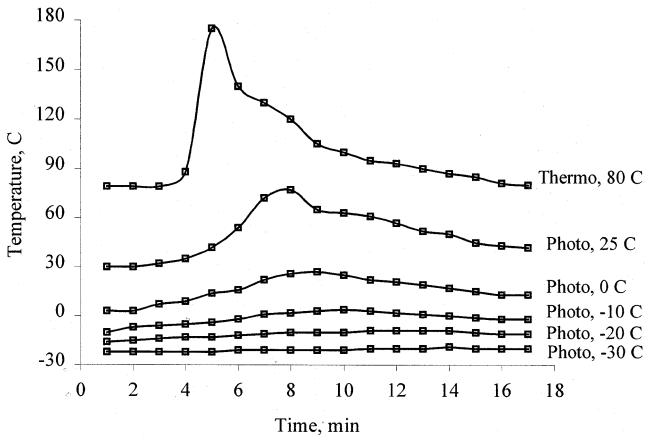

Figure 1. Temperature profile of the polymerization reaction. The plots begin 2 min before the start of gelation.

Table 1. Polymerization Conditions and Properties of the Imprinted Polymers

polymer	T_{init}, °C	T_{max}, °C	BET surf. area, $m^2\ g^{-1}$	total pore vol, $cm^3\ g^{-1}$	av pore diam, nm
MIP1	+80	+187	96.2	0.22	8.3
MIP2	+25	+78	15.8	0.028	6.9
MIP3	0	+27	1.9	0.004	7.2
MIP4	−10	+4	1.4	0.004	11.2
MIP5	−20	−10	0.9	0.002	10.8
MIP6	−30	−19	1.5	0.004	10.0
blank1	+80	+190	91.3	0.26	11.3
blank6	−30	−20	2.8	0.01	12.5

beneficial due to a reduction of the influence of residual vibrational modes (ΔG_{vib}) and an increase in the strength of polar interactions ($\sum \Delta G_p$)[8] (eq 1). At the same time the tighter complexes formed at lower temperature could be responsible for an increase in adverse conformational (ΔG_{conf}) and unfavorable van der Waals (ΔG_{vdW}) terms in eq 1.

It is surprising that only relatively limited efforts have been devoted to the analysis of the role of the polymerization temperature on complexation and recognition processes. To date, reported studies of this type include comparative analysis of the affinity, specificity, and adsorption capacity of the polymers prepared using thermal and photoinitiated polymerization.[9] O'Shannessy et al. compared sets of MIPs prepared at temperatures ranging from 0 to 60 °C using three different initiators and showed that polymers prepared at low temperature have better specificity compared to those prepared at higher temperature.[10] Since the initiators used in this study were different and this could lead to different morphology of the synthesized polymers, the interpretation of the temperature effect on polymer performance remains ambiguous. Additionally, the polymerization temperature was not recorded in these studies, although it might be expected that due to the exothermic character of the reaction, the real temperature in the polymerization mixture is higher than the one used to initiate the polymerization.

In this work we have carried out chromatographic analysis of polymers prepared at different temperatures and made an attempt to analyze the energetics, which control the molecular recognition in imprinted polymers. The mechanisms and thermodynamic origin of the chiral recognition displayed by the MIPs are discussed.

Results and Discussion

To analyze the impact of polymerization temperature on MIPs affinity and specificity, a set of polymers, imprinted with (−)-ephedrine at six different temperatures, −30, −20, −10, 0, 20, and 80 °C, was prepared using the same monomer composition (see Experimental Section). The polymer performance was analyzed in chromatographic experiments.

The temperature of the polymerization mixture was monitored using a thermocouple (Figure 1). As one might expect, the real polymerization temperature, due to the exothermic nature of the process, was significantly higher than the one used for initiation of the reaction (Table 1). The rate of the polymerization reaction was slower at low temperatures. Better control of the reaction at lower temperatures was probably responsible for the production of more homogeneous, gel-like materials with a decreased surface area, pore volume, and swellability in chloroform (Tables 1 and 3).

In theory, the polymerization temperature can affect the polymer morphology in different ways due to complexity of the process of phase separation. The free-radical initiator decomposes, generating free radicals and forming cross-linked nuclei or domains, which soon become insoluble and precipitate in the reaction medium forming globules. On one hand, the higher polymerization temperatures lead to the formation of a larger number of free radicals and a larger number of growing nuclei and globules. The formation of a larger number of globules at higher temperature is compensated by their smaller size. The polymer composed of smaller globules will have a larger number of smaller pores and larger surface area. On the other hand, temperature also affects the phase separation of the polymers from solution through the solvation of forming nuclei. Normally an increase in temperature improves the nuclei solubility. Therefore, at higher temperature the precipitating nuclei will have a higher molecular weight. As a result, both the nuclei and the voids between them would be larger.[11] Obviously, an increased surface area and pores volume for the polymers MIP1 and MIP2 serves as an indication that the first process plays a more important role in determining their morphology.

The polymerization temperature for polymers MIP 1 and MIP 2 reached relatively high values (187 and 78 °C, respectively) (Table 1). These conditions might be unsuitable for imprinting of thermally sensitive templates which could decompose, and natural molecules, such as proteins and nucleic acid, which denature at elevated temperatures.

Table 2. Thermodynamic Parameters for Polymers[a]

polymer	ΔH_{app}(50 °C), kcal mol^{-1}	ΔS_{app}(50 °C), cal $mol^{-1}\ K^{-1}$	ΔH_{app}(0 °C), kcal mol^{-1}	ΔS_{app}(0 °C), cal $mol^{-1}\ K^{-1}$
MIP1 (−)-ephedrine	−2.8	−7.7	−0.02	1.4
MIP1 (+)-ephedrine	−3.4	−10.4	−0.5	−0.7
MIP6 (−)-ephedrine	−5.8	−13.9	4.4	21.4
MIP6 (+)-ephedrine	−3.8	−9.3	2.4	12.0

[a] The enthalpies (ΔH_{app}) and entropies (ΔS_{app}) were obtained from linear regression of the linear parts of the corresponding Van't Hoff plots of ln K' vs $1000/RT$.

Table 3. Swelling Ratio of the Polymers[a]

polymer	swelling ratio chloroform	swelling ratio chloroform + HMDA	swelling ratio chloroform + HMDA + (−)-ephedrine (1 mg mL^{-1})
MIP1	2.33 ± 0.02	2.33 ± 0.04	2.37 ± 0.02
blank1	2.20 ± 0.04	2.19 ± 0.02	2.20 ± 0.01
MIP2	1.86 ± 0.03	1.82 ± 0.03	1.87 ± 0.03
MIP3	1.77 ± 0.02	1.76 ± 0.02	1.81 ± 0.02
MIP4	1.72 ± 0.03	1.71 ± 0.05	1.77 ± 0.02
MIP5	1.78 ± 0.05	1.77 ± 0.05	1.86 ± 0.03
MIP6	1.77 ± 0.03	1.75 ± 0.01	1.86 ± 0.03
blank6	1.72 ± 0.01	1.71 ± 0.01	1.72 ± 0.02

[a] Swelling ratio = amount of solvent adsorbed/dry weight of the polymer.

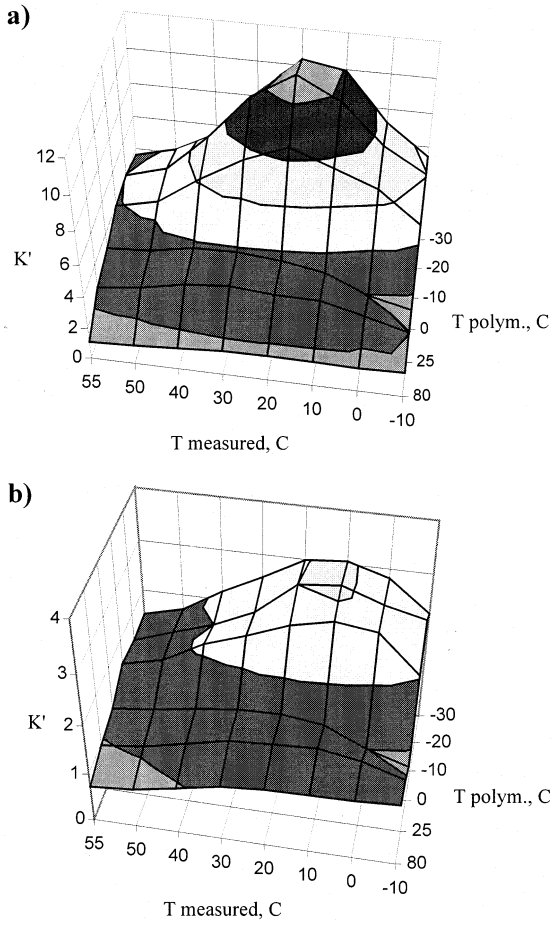

Figure 2. Influence of the polymerization temperature on capacity factors (*K′*) for (−)-ephedrine (a) and (+)-ephedrine (b) measured at different temperatures. Flow rate = 1 mL min^{-1}; mobile phase = 0.05% HMDA in chloroform. Injection amounts were 8 μg (48.5 nmol) in 40 μL injection volume.

The chromatographic evaluation of synthesized polymers was performed at eight temperatures: −10, 0, 10, 20, 30, 40, 50, and 55 °C. The results of this evaluation, expressed in terms of temperature dependence of capacity and separation factors for ephedrine enantiomers, are presented in Figures 2a,b and 3.

As expected, a clear increase in capacity (*K′*) and separation factors (α) with decrease in polymerization temperature was observed (see the chromatograms in Figure 4a,b). This effect was more pronounced for the template (−)-ephedrine than (+)-ephedrine which resulted in a large increase from α = 1.53 for MIP 1 to α = 4.04 for MIP5. No additional increase in polymer specificity and affinity was observed when the polymerization temperature was decreased further from −20

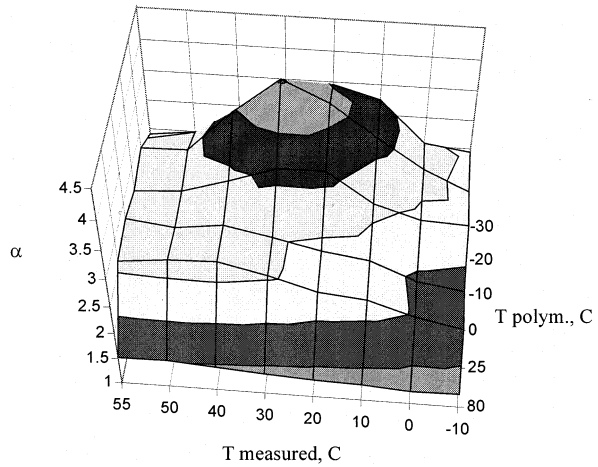

Figure 3. Influence of the polymerization temperature on separation factors (α) for MIP1−MIP6 measured at different temperatures. Flow rate = 1 mL min^{-1}; mobile phase = 0.05% HMDA in chloroform. Injection amounts were 8 μg (48.5 nmol) in 40 μL injection volume.

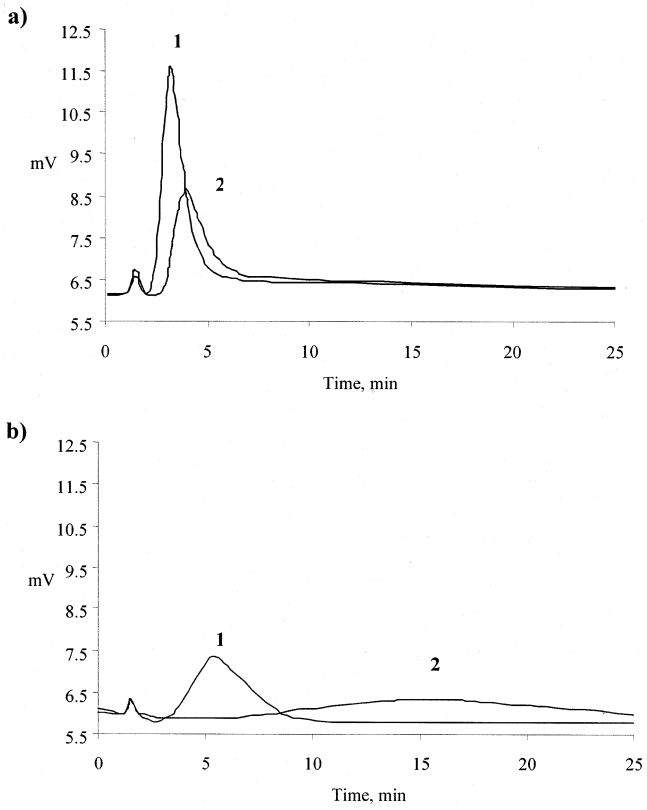

Figure 4. Chromatograms of (+)-ephedrine (1) and (−)-ephedrine (2) on MIP1 (a) and MIP 6 (b). Flow rate = 1 mL min^{-1}; mobile phase = 0.05% HMDA in chloroform; temperature = +30 °C. Injection amounts were 8 μg (48.5 nmol) in 40 μL injection volume.

°C (MIP5) to −30 °C (MIP6). The binding constants for polymers MIP 1 and MIP 6 were calculated using frontal analysis (performed at 30 °C) which allows the accurate determination of adsorption data from breakthrough experiments.[12] The binding isotherms for both polymers could be fitted with a Langmuir binary site model. The polymer synthesized at low temperature has a similar number of high affinity binding sites to the polymer prepared at higher temperature (Bt = 2.05 μmol g^{-1} for MIP1 and Bt = 2.23 μmol g^{-1} for MIP6) but had higher affinity (K_D = 0.32 mM for MIP 1 and K_D = 0.11 mM

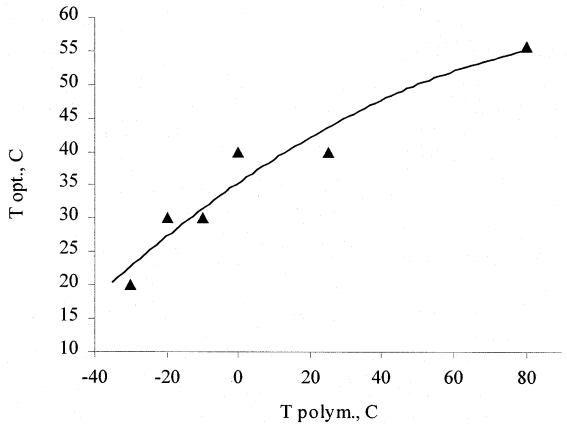

Figure 5. Temperature optimum of polymer specificity (α) vs polymerization temperature for MIP1−MIP6.

for MIP6). The number of low affinity binding sites was significantly smaller for MIP6 as compared with MIP1 (Bt = 8.45 μmol g^{-1} for MIP6 and Bt = 27.6 μmol g^{-1} for MIP1), but again, their affinity was higher (K_D = 1.64 mM for MIP6 and K_D = 4.17 mM for MIP 1).

The role of the temperature on column performance in enantioseparation has been studied previously. Depending on the experimental conditions, the affinity of polymers in enantioseparation was found to increase or decrease at elevated temperature.[14] It is interesting that with increase in temperature of separation in this study (with the exception of MIP1) the polymers affinity and enantioseparation improved initially, reaching a maximum at 10−30 °C, and then declined at higher temperatures. With a decrease in polymerization temperature the optimum enantioseparation also shifted to a lower temperature (Figure 5).

From past experiments a general observation for imprinted polymers is that optimum binding occurs when the polymer is exposed to the same conditions as those used for polymerization. Thus, a MIP often has optimal binding in the same solvent in which it was polymerized.[13] The reason for this lies in the postulated mechanism of template recognition by a MIP, which originates, basically, from two factors: shape of the imprints and the spatial positioning of the functional groups in the polymer which are participating in the complex with the template and are integrated into the polymer network during the polymerization stage. The distance between these groups and their orientation in the polymer can be affected by a swelling process, and because of this, the MIP can lose its specificity when immersed in the "wrong" solvent. We might also expect that during the polymerization stage the microenvironment of the developing imprints adjusts to the solvation by the porogen at a certain temperature. As a result, the polymer will "memorize" the temperature developed during polymerization. It is important to note that in this work only an indication of a connection between the measured temperature of polymerization reaction and optimum polymer performance has been observed, not a direct correlation. The reason for this lies in the complex nature of the recognition process. For example, binding at low temperature will depend significantly on mass transfer, which will obviously be slow at low temperature, thus preventing effective recognition of the template by the MIP.

The determination of thermodynamic parameters is a crucial tool in the characterization of polymer−

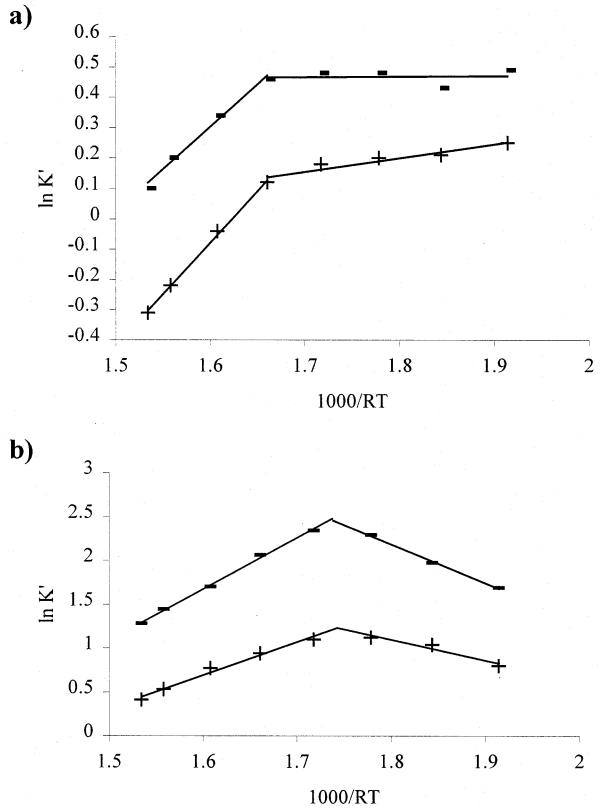

Figure 6. Van't Hoff plots of the capacity factors (K') for 48.5 nmol of ephedrine enantiomers on MIP1 (a) and MIP6 (b). Flow rate = 1 mL min^{-1}; mobile phase = 0.05% HMDA in chloroform; (−) = (−)-ephedrine; (+) = (+)-ephedrine.

template interactions. Chromatographic retention data from variable-temperature runs may be used to evaluate thermodynamic properties according to the Van't Hoff equation.[15] This approach can offer an insight into the nature of the interaction between the template and polymer and help to elucidate the chemical forces underlying the interactions.

Figure 6 shows the plots of ln K' vs 1000/RT in a mobile phase containing 0.05% of hexamethylenediamine as additive. The plots for polymers MIP1 and MIP6 indicate two intersected linear parts with different slopes. The correlation coefficients for the fits were at least equal to 0.94. The linear portions of these plots were fitted by linear regression analysis, giving values assigned as apparent ΔH_{app} and ΔS_{app}. Table 2 contains a list of ΔH_{app} and ΔS_{app} values for MIP1 and MIP6. The major change in the slopes of Van't Hoff plots observed at 20−30 °C is thought to be associated with a change in mechanism of binding from exothermic to endothermic at this temperature. At higher temperatures (>20 °C) the binding process is exothermic. A negative enthalpy suggests interactions such as hydrogen-bonding, ion-pairing, and van der Waals interactions. It is noteworthy that the value of the apparent ΔH for the template−MIP6 interaction at temperatures >20 °C (−7.06 kcal mol^{-1}) was approximately 2 times larger than that for the (+)-ephedrine−MIP6 interaction (−3.69 kcal mol^{-1}) and 2 times larger than that for the (±)-ephedrine−MIP1 interaction. This could potentially arise from MIP6 forming a higher ordered complex with the template; for example, two monomers might react with one template molecule under these conditions.

For the MIPs prepared at lower temperatures the larger enthalpy gains are thought to be associated with

larger entropy losses. Inclusion of the template into a tighter binding site with its restricted size and shape greatly reduces the template's freedom, giving more negative entropic contributions. The negative entropy at temperatures higher than 20 °C observed for all MIPs indicates an increase in the order of the chromatographic system as the solute was bound by the polymer. This is a result of an energetic penalty associated with the freezing of a rotor ΔG_r (eq 1). The value of $T\Delta S = 3-4.5$ kcal mol^{-1} (MIP1 and MIP6 at 50 °C) is only 2−3 times higher than the value $T\Delta S = 1-1.4$ kcal mol^{-1} per rotor calculated for weak complexes.[16] Assuming that at 50 °C the binding sites have an open conformation and desolvation effects are minimal, it is possible to conclude that only a small part of the template molecule (∼1/3) is embedded into the binding cavity; otherwise, the energetic penalty will be larger.

The binding of both enantiomers at lower temperatures (<20 °C) is exclusively entropy-driven, and positive entropy gains even outweigh unfavorable enthalpy changes. Entropy-driven binding and recognition have been frequently observed for MIPs, inclusion complexes, and natural receptors.[15,17] The most likely scenario is that the template molecule induces a more extensive rearrangement and displacement of solvent molecules from the imprint, which involves changes in solvation of both the host polymer binding site and the guest molecule. The breaking of hydrogen or van der Waals bonds formed between the polymer chains leads to the imprint assuming a more open configuration so there is greater freedom of movement in the polymer functional groups and polymer−template complex. It is logical to assume that this effect is stronger for the (−)-ephedrine−template than for (+)-ephedrine, and this is reflected in a more positive entropy term.

To study this model, swelling experiments were performed in the presence and absence of the template (Table 3). A clear increase in swelling was observed in the presence of template. This effect was more pronounced in the case of the polymer prepared at low temperature (MIP6). The magnitude of template-induced swelling was lower in this work when compared to that previously observed for MIPs with a low levels of cross-linking.[18] It is important to note that template-induced changes in the polymer conformation are system-dependent. Depending on the type of interactions between the polymer chains and interactions of the polymer chains with solvent molecules, the template can increase swelling, as in the current case, produce no changes at all, or decrease swelling.[7,19] In water, for example, we might expect strong competition from water molecules in hydrogen bonding to the polar polymer chains, which will prevent their self-association. Because of osmotic pressure, the size of imprinted cavities will most likely increase upon release of the template. The template, during the rebinding step, will displace water molecules, inducing shrinking of the polymer.[18] The template-induced changes in polymer conformation can be used for the development of supramolecular devices that could transform a binding event into a detectable electrical signal.[20]

Besides the binding thermodynamics, temperature will also affect transport and binding kinetics. Thus, the increased viscosity of the mobile phase at low temperature can affect the separation efficiency due to the reduced rate of mass transfer in solution and on the binding sites. This effect can be quantified using Van Deemter analysis.[21] The detailed analysis, however, required measurements performed at different flow rates, which was difficult to achieve due to excessive broadening of the peak shape at flow rates below 0.5 mL/min and too high back pressure at flow rates above 2 mL/min.

Conclusion

The present results indicate that the polymerization temperature plays a crucial role in the performance of the synthesized materials. The polymer's affinity and specificity were significantly improved by decreasing the polymerization temperature. The presence of a temperature-dependent optimum in polymer performance illustrates how a polymer can "memorize" the temperature used in polymerization, in a manner similar to previously documented memory effects existing in MIP systems for the template and polymerization solvent. Analysis of the thermodynamic parameters of the polymer−template interaction shows that the template binding by the synthesized MIP at low temperature in contrast to binding at higher temperature is most likely entropy driven, resulting from a release of solvent molecules from the cavities and from the conformational changes in polymer induced by the template. This study indicates the principal possibility of modulating the polymer's properties by optimizing the temperature regime and shows the importance of a thermodynamic analysis for a better understanding of the nature of molecular recognition in MIP systems.

Experimental Section

Chemicals. (1*R*,2*S*)-Ephedrine ((−)-ephedrine) and (2*R*,1*S*)-ephedrine ((+)-ephedrine) were supplied by Chemical Development, GlaxoSmithKline R&D, UK. Ethylene glycol dimethacrylate (EGDMA), 2-hydroxyethyl methacrylate (HEM), 1,1′-azobis(cyclohexanecarbonitrile), hexamethylenediamine (HMDA), and chloroform were purchased from Aldrich (UK). All chemicals and solvents were analytical or HPLC grade and were used without further purification.

Preparation of Molecularly Imprinted Polymers. A set of polymers was synthesized at different polymerization temperatures (Table 2). A 10:1 molar ratio of functional monomers to template was used in order to saturate all functional binding sites in the template. To a solution of (−)-ephedrine (1.21 mmol, 0.2 g) in chloroform (8.82 g) was added 2-hydroxyethyl methacrylate (12.1 mmol, 1.57 g), ethylene glycol dimethacrylate (35.9 mmol, 7.1 g), and 1,1′-azobis(cyclohexanecarbonitrile) (0.18 g). The monomer mixture was placed into a 50 mL glass tube, purged with nitrogen for 5 min, and sealed. The bottles were placed in a thermostat (LTD20G, Grand Instruments, Cambridge, UK) and equilibrated for 20 min at temperatures ranging from −30 to +80 °C. The polymerization was initiated by heating at 80 °C (MIP 1) or photochemically (MIP2-MIP6) using a fiber-optic light source with a 300 W CERMAX xenon arc lamp (PerkinElmer Optoelectronics, Inc.) for 3 h duration of exposure. During this time the samples were rotated periodically to ensure even polymerization. Corresponding blank polymers were prepared in the absence of the template. The bulk polymers were ground in methanol with an electrical mortar SL2 (Silverson, UK) and mechanically wet-sieved through 38 μm sieves (Endecotts, UK) and sedimented in methanol to remove fines. The polymers were additionally washed out with chloroform containing 0.05% hexamethylenediamine. Spectrophotometric analysis of ephedrine concentration in washing solutions performed at 260 nm indicates that 94−95% of the template was removed successfully from the polymer. Polymer particles were collected, dried under vacuum, and used for packing HPLC columns.

The determinations of specific surface area were performed using an ASAP 2000 instrument (Micrometrics Instrument Corp.) based on the nitrogen BET.

HPLC Analysis. For the analysis of MIP's recognition properties the polymer particles were suspended in methanol and packed in a stainless steel HPLC columns (150 × 4.6 mm) under reduced pressure. The evaluation experiments were carried out using an HPLC system, which included a Consta-Metric-3200 solvent delivery system (LDC Analytical, UK), a Perkin-Elmer ISS-100 automatic injection system, and a Waters Lambda-Max model 481 LC detector (UK). The temperature of the column and eluent was maintained constant within ±0.1 °C, using a thermostat (LTD20G, Grand Instruments, Cambridge, UK). Columns were washed with 0.05% hexamethylenediamine in chloroform at a constant flow (1 mL min^{-1}) until a stable baseline was achieved. HPLC analysis was performed at a flow rate of 1.0 mL min^{-1} and monitored by UV detector at 260 nm. Injection amounts were 8 μg (48.5 nmol) in 40 μL injection volume. The affinity of ephedrine enantiomers was examined at the temperature values of −10, 0, 10, 20, 30, 40, 50, and 55 °C. The chromatographic system was allowed to equilibrate at each temperature for at least 1 h prior to each experiment. All reported chromatographic data represent the results of 3−5 concordant experiments. The standard deviation of the measurements was below 5%.

Capacity Factors, Separation Factors, and Van't Hoff Plot. Capacity factors (K') were determined from $K' = (t - t_0)/t_0$, where t is the retention time of a given species and t_0 is the retention time of the void marker (acetone). Effective enantioseparation factors (α) were calculated from the relationship $\alpha = K'(-)/K'(+)$, where $K'(-)$ and $K'(+)$ are the capacity factors of the (−)- and (+)-ephedrine, respectively.

The capacity factor K' is proportional to equilibrium dissociation constant K and can be written as

$$K' = \phi K \tag{2}$$

where ϕ is the phase ratio (volume of the stationary phase divided by volume of mobile phase). It was calculated from the dead volume and sum of the dead volume with disconnected column and geometrical volume of the column. The value obtained varies depending on the material and the temperature, e.g., $\phi = 0.76 \pm 0.02$ for MIP1, $\phi = 0.63 \pm 0.02$ for MIP5, and 0.52 ± 0.01 for MIP6. The temperature variations were about 4%.

The change in the standard Gibbs free energy ($\Delta G°$) is related to the equilibrium constant by the equation

$$\Delta G° = -RT \ln K \tag{3}$$

The relation between change in free energy and change in enthalpy and entropy can be described by the equation

$$\Delta G° = \Delta H° - T\Delta S° \tag{4}$$

$\Delta H°$ is the enthalpy and $\Delta S°$ is the entropy of transfer of the solute from the mobile phase to the stationary phase, T is the temperature, and R is the gas constant. Combining eqs 2 and 4, the capacity factor can be expressed by the integrated form of the Van't Hoff equation:

$$\ln K' = -(\Delta H°/RT) + (\Delta S°/R) + \ln \phi \tag{5}$$

From the slope and the intercept, $-\Delta H_{app}$ and $(\Delta S_{app}/R) + \ln \phi$ respectively were calculated. The ΔH_{app} and ΔS_{app} should be considered as apparent, since the phase ratio (ϕ) is also dependent on the temperature.

Swelling Analysis. Swelling experiments were performed as described previously.[22] 300 mg of the polymer particles with the mesh size 38−67 μm was packed in 1 mL solid-phase extraction cartridges (Supelco, UK). Cartridges were filled with 1 mL of chloroform, 0.05% solution of HMDA in chloroform, and a solution of 1 mg mL^{-1} (−)-ephedrine in 0.05% HMDA in chloroform. After 6 h equilibration at 20 °C the excess of solvent was removed from the polymer by applying reduced pressure for 1 min, and the weight of the swollen polymer was measured. The swelling ratio (Sr) of the polymers was calculated from the following equation:

$$\mathrm{Sr} = (m_s - m_0)/m_0 \tag{6}$$

where m_s is the mass of the swollen polymer and m_0 is the mass of dry polymer.

References and Notes

(1) (a) Allen, W. E.; Gale, P. A.; Brown, C. T.; Lynch, V. M.; Sessler, J. L. *J. Am. Chem. Soc.* **1996**, *118*, 12471−12472. (b) Wang, Y.; Bluhm, L. H.; Li, T. *Anal. Chem.* **2000** *72*, 5459−5465. (c) Hart, B. R.; Rush, D. J.; Shea, K. J. *J. Am. Chem. Soc.* **2000**, *122*, 460−465.

(2) Wulff, G.; Sarhan, A. *Angew. Chem., Int. Ed. Engl.* **1972**, *11*, 341−344.

(3) Holroyd, S. E.; Groves, P.; Searle, M. S.; Gerhard, U.; Williams, D. H. *Tetrahedron* **1993**, *49*, 9171−9182.

(4) (a) Nicholls, I. A. *Chem. Lett.* **1995**, 1035−1036. (b) Nicholls, I. A.; Adbo, K.; Andersson, H. S.; Andersson, P. O.; Ankarloo, J.; Hedin-Dahlström, J.; Jokela, P.; Karlsson, J. G.; Olofsson, L.; Rosengren, J.; Shoravi, S.; Svenson, J.; Wikman, S. *Anal. Chim. Acta* **2001**, *435*, 9−18.

(5) (a) Piletsky, S. A.; Day, R. M.; Chen, B.; Subrahmanyam, S.; Piletska, O.; Turner, A. P. F. PCT/GB01/00324, 2001. (b) Piletsky, S. A.; Karim, K.; Piletska, E. V.; Day, C. J.; Freebairn, K. W.; Legge, C.; Turner, A. P. F. *Analyst* **2001**, *126*, 1826−1830.

(6) (a) Wulff, G. *Angew. Chem., Int. Ed. Engl.* **1995**, *34*, 1812−1832. (b) Yu, C.; Mosbach, K. *J. Chromatogr. A* **2000**, *888*, 63−72.

(7) Sellergren, B.; Shea, K. J. *J. Chromatogr. A* **1993**, *635*, 31−49.

(8) (a) Bruyneel, C.; Zeegers-Huyskens, Th. *J. Mol. Struct.* **2000**, 177−185. (b) Steinke, J. H. G.; Dunkin, I. R.; Sherrington, D. C. *Trends Anal. Chem.* **1999**, *18*, 159−163.

(9) (a) Sellergren, B.; Lepisto, M.; Mosbach, K. *J. Am. Chem. Soc.* **1988**, *110*, 5853−5860. (b) O'Shannessy, D. J.; Ekberg, B.; Andersson, L. I.; Mosbach, K. *J. Chromatogr.* **1989**, *470*, 391−399.

(10) O'Shannessy, D. J.; Ekberg, B.; Mosbach, K. *Anal. Biochem.* **1989**, *177*, 144−149.

(11) Viklund, C.; Svec, F.; Frechet, J. M. J. *Chem. Mater.* **1996**, *8*, 744−750.

(12) Andersson, H. S.; Koch-Schmidt, A.-C.; Ohlson, S.; Mosbach, K. *J. Mol. Recognit.* **1996**, *9*, 675−682.

(13) (a) Wulff, G.; Pol, H.-G.; Minarik, M. *J. Liq. Chromatogr.* **1986**, *9*, 385−405. (b) Haginaka, J.; Sanbe, H. *J. Chromatogr. A* **2001**, *913*, 141−146. (c) Allender, C. J.; Heard, C. M.; Brain, K. R. *Chirality* **1997**, *9*, 238−242.

(14) (a) Spivak, D.; Gilmore, M. A.; Shea, K. J. *J. Am. Chem. Soc.* **1997**, *119*, 4388−4393. (b) Yu, C.; Mosbach, K. *J. Chromatogr. A* **2000**, *888*, 63−72.

(15) (a) Sellergren, B.; Shea, K. J. *J. Chromatogr. A* **1995**, *690*, 29−39. (b) Guillaume, M.; Jaulmes, A.; Sebille, B.; Thuaud, N.; Vidal-Madjar, C. *J. Chromatogr. B* **2001**, *753*, 131−138.

(16) Searle, M. S.; Williams, D. H. *J. Am. Chem. Soc.* **1992**, *114*, 10690−10697.

(17) (a) Morin, N.; Guillaume, Y. C.; Peyrin, E.; Rouland, J.-C. *J. Chromatogr. A* **1989**, *808*, 51−60. (b) Li, J.-G.; Raffa, R. B.; Cheung, P.; Tzeng, T.-B.; Liu-Chen, L.-Y. *Eur. J. Pharmacol.* **1998**, *354*, 227−237. (c) Borea, P. A.; Bertelli, G. M.; Gilli, G. *Eur. J. Pharmacol.* **1998**, *146*, 247−252.

(18) Watanabe, M.; Akahoshi, T.; Tabata, Y.; Nakayama, D. *J. Am. Chem. Soc.* **1998**, *120*, 5577−5578.

(19) Wolfbeis, O. S.; Terpetschnig, E.; Piletsky, S.; Pringsheim, E. In *Applied Fluorescence in Chemistry, Biology and Medicine*; Rettig, W., Strehmel, B., Schrader, S., Seifert, H., Eds.; Springer: Berlin, 1998; pp 277−295.

(20) (a) Piletsky, S. A.; Piletskaya, E. V.; Panasyuk, T. L.; El'skaya, A. V.; Levi, R.; Karube, I.; Wulff, G. *Macromolecules* **1998**, *31*, 2137−2140. (b) Sergeyeva, T. A.; Piletsky, S. A.; Brovko, A. A.; Slinchenko, E. A.; Sergeeva, L. M.; Panasyuk, T. L.; El'skaya, A. V. *Analyst* **1999**, *124*, 331−334. (c) Yoshimi, Y.; Ohdaira, R.; Iiyama, C.; Sakai, K. *Sens. Actuators B* **2001**, *73*, 49−53.

(21) Knox, J. H. *J. Chromatogr. A* **2002**, *960*, 7−18.

(22) Sarayadin, D.; Karadag, E.; Caldiran, Y.; Güven, O. *Radiat. Phys. Chem.* **2001**, *60*, 203-210.

MA0205562